DOI: 10.1002/cssc.201200173

Quasi-Homogeneous Oxidation of Glycerol by Unsupported Gold Nanoparticles in the Liquid Phase

Elżbieta Skrzyńska,*[a, b, c] Jamal Ftouni,[b, c] Jean-Sébastien Girardon,[b, c] Mickaël Capron,[b, c] Louise Jalowiecki-Duhamel,[b, c] Jean-François Paul,[b, c] and Franck Dumeignil*[b, c, d]

A quasi-homogeneous solution of gold nanoparticles prepared by the Turkevich method was used as an unconventional catalyst in the oxidation of glycerol (GLY) in the liquid phase. The highest obtained conversion was 100 % after 3 h of reaction at 100 °C under an oxygen atmosphere (5 bar). The main products were glyceric, glycolic, formic, tartronic, and oxalic acid with selectivities of 28, 36, 25, 9, and 2 %, respectively. Traces of hydroxypyruvic and acetic acid were also detected (combined selectivities below 1 %). To elucidate the reaction mechanism and specify the role of gold nanoparticles in the oxidation process, a series of experiments under various reaction conditions were carried out. The effect of reaction temperature, oxygen pressure, gold concentration, and GLY/base molar ratio was investigated. All catalytic results were systematically compared to the corresponding noncatalytic base-induced transformations (blank tests). Such an approach allowed us to separate and clarify the respective driving parameters for the transformation of GLY (presence of a base and activity of the gold catalyst). The reaction mechanism comprised a series of oxidation and C–C cleavage reactions, whereas additional oxidation–reduction reactions (of the Cannizzaro type) could also occur in the presence of the base.

Introduction

In the last decade, a lot of investigations have been focused on catalytic transformation of glycerol (GLY) to more valuable chemicals used directly as additives or as raw materials in a large number of industrial applications, including food/feed, self-care products and pharmaceuticals, manufacture of alkyd resins, polyurethanes and fuel additives, tobacco products, production of varnishes, adhesives, explosives, etc.[1–8]

Biochemical pathways, pyrolysis, reforming, reduction, esterification, etherification, cyclization, halogenation, and condensation reactions have been used for the transformation of GLY. However, the catalytic oxidation of GLY in the liquid phase has attracted great interest lately.[1–3,6–10] The majority of work in the field of GLY partial oxidation is based on the use of platinum-, palladium-, and, more recently, gold-supported catalysts. The issues of activating GLY under moderate reaction conditions imposed by the use of the liquid phase were raised, and the influence of parameters such as GLY concentration, pH, reaction temperature, and oxygen pressure was analyzed. Importantly, the studies focused on the investigation of the effect of the physicochemical properties of metal-based supported catalysts (mainly Pd, Pt, or Au typically deposited on carbon, silica, or alumina supports) on catalytic performance. A recent review[1] points out that gold-based catalytic systems seem to be the most promising among all catalytic systems proposed so far in the literature due to their higher stability.

In the case of gold-catalyzed GLY oxidation, it has been claimed that the addition of a base in the reaction medium is necessary for the initial step of GLY activation, which leads to the abstraction of an H^+ from an OH moiety.[1] The main reaction conditions used by various studies are similar: in most cases, the GLY/base molar ratio is equal to 1 or 4, whereas GLY concentration rarely exceeds 20 wt %. Furthermore, most studies use a GLY/Au molar ratio of up to 3500, irrespective of the dispersion of the active phase, which is directly connected with the method of preparation and the size of Au particles. Moreover, most processes operate at moderate temperatures of around 60 °C and under an oxygen atmosphere at a pressure of up to 10 bar. Despite the large number of studies on gold reactivity in GLY conversion, many aspects of the reaction need additional investigation. For example, there are only a few examples of studies dealing with quasi-homogeneous oxidations, in which unsupported “bare” or stabilized gold particles are used as catalysts,[11–14] especially in the oxidation of GLY.[15,16] Another aspect, also largely omitted in the literature, is the noncatalytic transformation of GLY in the liquid phase under basic conditions. Indeed, the so-called “blank tests”

---

[a] Dr. E. Skrzyńska
Faculty of Chemical Engineering and Technology
Cracow University of Technology
Ul. Warszawska 24, 31-155 Cracow (Poland)
E-mail: eskrzynska@pk.edu.pl

[b] Dr. E. Skrzyńska, J. Ftouni, Dr. J.-S. Girardon, Dr. M. Capron,
Dr. L. Jalowiecki-Duhamel, Prof. J.-F. Paul, Prof. F. Dumeignil
CNRS UMR8181, Unité de Catalyse et Chimie du Solide
UCCS, 59655 Villeneuve d’Ascq (France)
E-mail: franck.dumeignil@univ-lille1.fr

[c] Dr. E. Skrzyńska, J. Ftouni, Dr. J.-S. Girardon, Dr. M. Capron,
Dr. L. Jalowiecki-Duhamel, Prof. J.-F. Paul, Prof. F. Dumeignil
Univ. Lille Nord de France
59000, Lille (France)

[d] Prof. F. Dumeignil
Institut Universitaire de France
Maison des Universités
10 Boulevard Saint-Michel, 75005 Paris (France)

(tests that are carried out without catalyst) are insufficiently described. In the case of GLY oxidation in the liquid phase, the presence of a base (e.g., NaOH) has a critical influence because it is commonly admitted that in its absence GLY cannot be activated over gold catalysts and no conversion can be expected. However, we additionally found that under specific conditions the presence of a base can promote some GLY transformations through pathways that are different from those described when using catalysts. Thus, our goal is to decouple the reactivity specifically due to the catalytic system (gold nanoparticles in the presence of a base) from that induced by the presence of a base alone.

Results and Discussion

Characterization of gold nanoparticles

UV spectroscopy characterization was primarily used to confirm the formation of gold nanoparticles (Au^0) and to estimate total consumption of the gold precursor ($HAuCl_4$). In UV/Vis spectra (Figure 1), the absence of a band at 300 nm, which is characteristic of the gold precursor (Au^{3+}), and the presence of a strong and well-defined surface-plasmon band at 525 nm in the final solution confirmed the metallic state of gold.[17]

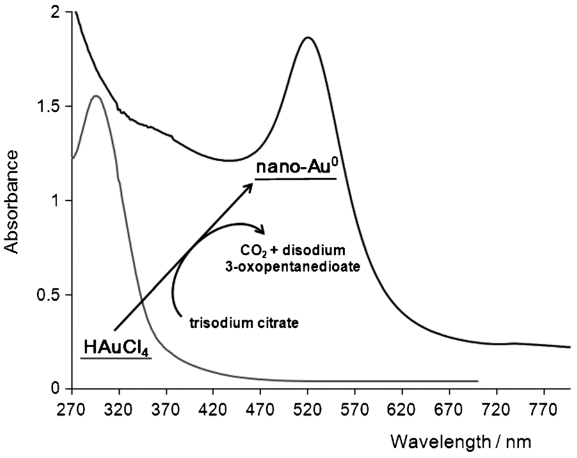

Figure 1. Typical UV/Vis spectra of the gold catalyst precursor ($HAuCl_4$) and gold nanoparticles obtained by the Turkevich method.

The reaction presented in Figure 1 can be expressed by the simplified Equation (1). However, the exact process is composed of a series of consecutive reactions.[18]

$$3\,(H_2CCOO^-)_2C(OH)COO^- + 2\,AuCl_4^- \rightarrow 3\,(H_2CCOO^-)_2C{=}O + 2\,Au + 8\,Cl^- + 3\,H^+ + 3\,CO_2 \tag{1}$$

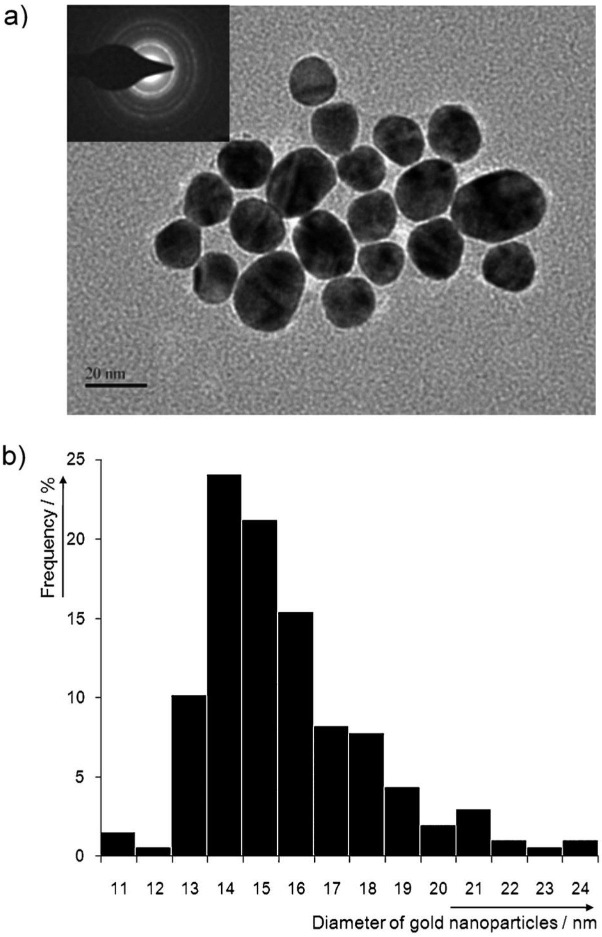

Figure 2. a) Representative TEM micrograph and SAED pattern and b) histogram of metal particle size distribution for the solution of gold nanoparticles.

In the literature it has been established that the shape of the absorption band and the maximum wavelength of absorbance depended strongly on the size of nanoparticles.[19,20] The spectrum presented in Figure 1 thus suggests the presence of gold nanoparticles with a diameter of about 15 nm. This was confirmed by means of TEM imaging (Figure 2a) and by statistical analyses of particle-size distribution of more than 250 particles, which indicated an average particle size of (16.2 ± 2.2) nm (Figure 2b), which is in good agreement with the literature.[21] To confirm the crystal structure of gold crystals as face-centered cubic, selected area electron diffraction (SAED) studies were undertaken (Figure 2a, inset).

Catalytic tests in a stainless steel reactor

First, the occurrence of parasitic side reactions that could be catalyzed by the stainless steel reactor itself was checked. We compared GLY oxidation performance in a glass reactor and in the routinely used stainless steel reactor under the same conditions (temperature, oxygen pressure, and reagent composition). At GLY isoconversion, the main product yields are comparable in both processes (Figure 3a and 3b, respectively). For example, in the stainless steel reactor, a GLY conversion of 10% was obtained after 100 min, and the yield in glyceric, glycolic, and formic acid was 1.7, 2.3, and 6.0%, respectively. Because of the differences in glass-reactor construction (absence of baffles and bigger reaction volume), the time necessary to obtain the same conversion was twice as long. Nevertheless, the yields recalculated by simple approximation were strictly

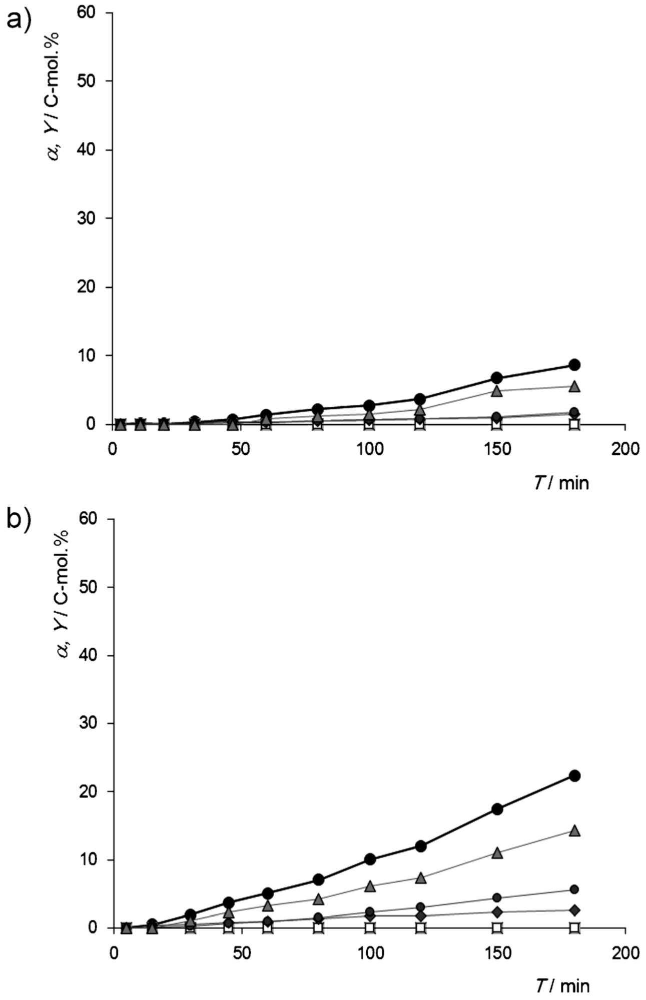

Figure 3. Comparison of GLY oxidation results [glycerol conversion (●) and yields of oxalic (⊠), tartronic (□), glyceric (◆), glycolic (●), and formic acid (▲)] for base-induced GLY transformation in a a) glass and a b) stainless steel reactor (blank tests). Reaction conditions: a) aq. GLY (300 mL, 0.3 M), NaOH/GLY = 4 (molar ratio), oxygen pressure: 2.8 bar, propeller speed: 1500 rpm, temperature inside the glass reactor and temperature of the oil bath: 60 °C, absence of baffles; b) aq. GLY (250 mL, 0.3 M GLY), NaOH/GLY = 4 (molar ratio), oxygen pressure: 2.8 bar, propeller speed: 1500 rpm, temperature inside the stainless steel reactor: 60 °C, 4 baffles.

identical (1.7, 2.3, and 6.0 % for glyceric, glycolic, and formic acid, respectively). The analogy between the processes was thus clear. Hence, we selected the stainless steel reactor for further catalytic tests because it provided better oxygen dispersion in the whole reaction volume and it allowed us to precisely adjust temperature and work under higher oxygen pressure.

Then, to separately be able to assess, on the one hand, the role of gold nanoparticles and, on the other hand, the role of the base (blank test), the amount of NaOH introduced to the reaction mixture, the amount of GLY/gold molar ratio, the oxygen pressure, and the reaction temperature were systematically varied in specific series of GLY partial oxidation experiments. Herein, we present the catalytic test results, sequentially focusing on the influence of each of the aforementioned parameters with a systematic comparison between the results obtained for the gold-catalyzed reaction and base-induced transformations.

Effect of NaOH/GLY molar ratio

The importance of the amount of base in catalytic and noncatalytic GLY transformations could be reliably evaluated by tests with different NaOH/GLY molar ratios (Figure 4).

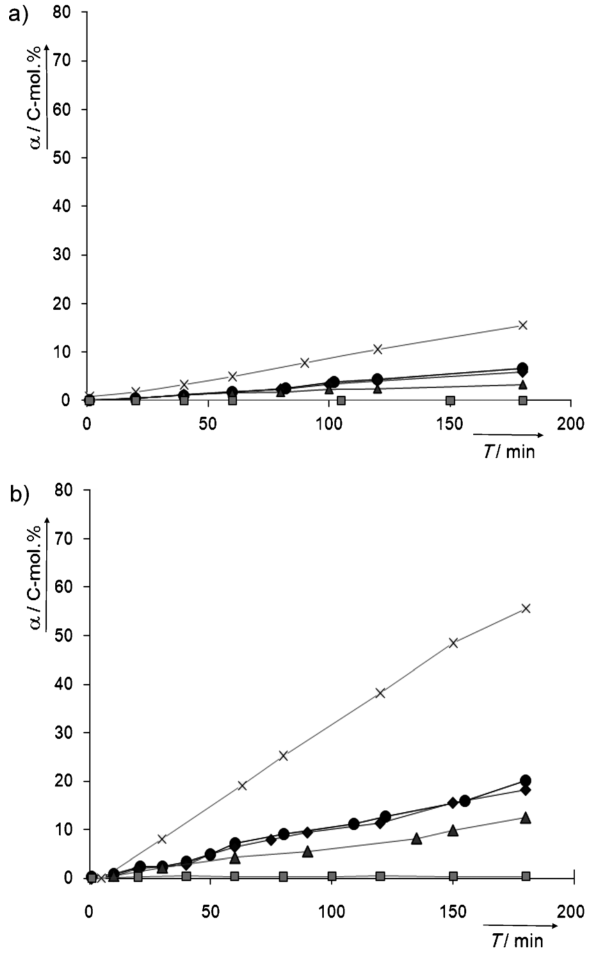

Figure 4. GLY conversion: Comparison between a) blank tests and b) GLY oxidation reactions in the presence of gold nanoparticles at NaOH/GLY molar ratios of 4 (×), 3 (●), 2 (◆), 1 (▲), and 0 (■). Reaction conditions: aq. GLY (200 mL, 0.3 M), NaOH/GLY = 0–4 (molar ratio), GLY/Au = 3500 (catalytic tests, molar ratio), oxygen pressure: 5 bar, temperature: 60 °C.

An increase in the concentration of NaOH strongly influenced GLY conversion. The results at NaOH/GLY ratios of 2 and 3 remained almost identical. An analogous effect was also observed by Suramanee et al.[15] for citrate-stabilized gold nanoparticles (reaction times of up to 3 h at 80 °C).

As expected, the most important feature of this experiment was that gold particles were not able to oxidize GLY without a base because conversion did not exceed 0.4 % after 3 h (Figure 4 b, NaOH/GLY = 0). Also, during noncatalytic tests without NaOH, we did not detect any conversion of GLY (Figure 4 a, NaOH/GLY = 0). Similar results for supported gold catalysts can be found in studies by Demirel-Gülen et al.[22] and Porta and Prati.[23] Those authors did not mention results for a NaOH/GLY ratio of 3.

Comparing the yields of the main products in blank and catalyst-assisted tests at a GLY conversion of 10% (Figure 5, derived from results in Figure 4) confirms that GLY conversion proceeds much faster in the presence of gold nanoparticles. Moreover, blank tests with different NaOH/GLY ratios give almost equivalent amounts of the main products (selectivity of about 30% towards glyceric, glycolic, and formic acid), whereas in the presence of catalyst, the main product is glyceric acid (>40%). An increase in the amount of base only slightly influences product distribution, again in favor of glyceric acid. In addition to glyceric, glycolic, and formic acid, small amounts of tartronic, hydroxypyruvic, and oxalic acid are also detected (Figure 5). Similar changes in main product distribution were previously observed by Porta and Prati[23] and Carrettin et al.[24] for carbon-supported gold catalysts.

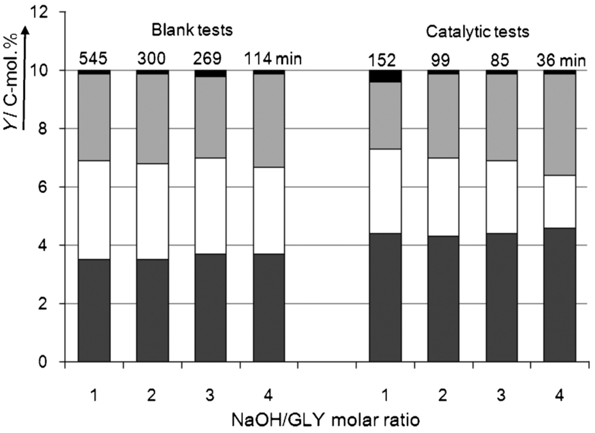

Figure 5. Comparison of main product yields [glyceric (■), glycolic (□), and formic acid (▨); tartronic, hydroxypyruvic, and oxalic acid have been summarized (■)] at a GLY conversion equal to 10% for tests with variable base concentrations. Reaction conditions are the same as those reported in Figure 3.

Effect of GLY/gold molar ratio

By comparing data from catalytic and noncatalytic tests (Figure 4 and 5), we can see that both conversion and glyceric acid productivity are lower in the absence of the gold catalyst. However, further changes in gold concentration (decrease or increase) do not significantly influence product selectivities, but clearly affect the overall reaction rate (i.e., GLY conversion increased with an increase in gold concentration; Figure 6).

An analogous relationship between the GLY/gold molar ratio and GLY conversion using an Au/C solid catalyst was previously reported by Gallezot,[25] who found that the reaction rate depended on catalyst concentration for GLY/gold ratios above 2500.

In Figure 6, we can see that GLY conversion after 1, 2, or 3 h increased with the increase in gold concentration. Conversely, for the same GLY conversion, the yield of glyceric, glycolic, and formic acid for each catalytic test only changed within a narrow range (Figure 7), with average values of 4.7–5.8, 1.6–2.5, and 2.2–3%, respectively. A lower productivity of glyceric acid was observed for the blank test (absence of gold), in which the yield values for each acid were comparable (3–3.8%).

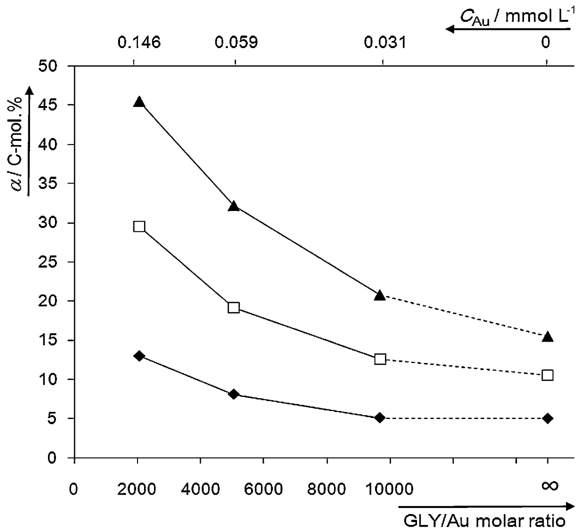

Figure 6. Changes in GLY conversion as a function of the GLY/gold molar ratio and reaction time [60 (◆), 120 (□), and 180 min (▲)]. Reaction conditions: aq. GLY (200 mL, 0.3 M), 60 °C, oxygen pressure: 5 bar, NaOH/GLY = 4 (molar ratio).

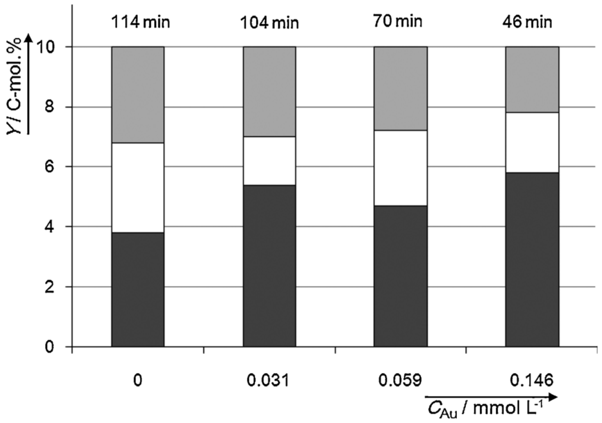

Figure 7. Comparison of main product yields [glyceric (■), glycolic (□), and formic acid (▨)] at a GLY conversion equal to 10% for tests with different concentrations of gold nanoparticles. The reaction conditions are the same as those in Figure 5.

Because the time necessary to obtain a GLY conversion of 10% decreased with an increase in the concentration of gold nanoparticles, for further catalytic tests the amount of gold was adjusted to 0.065 mmol L^{-1}, which corresponded to a GLY/gold molar ratio of 3500. This value was a good compromise between the amount of catalyst used and the observed reaction rate.

Effect of oxygen pressure

The next important parameter was oxygen pressure. Experiments were designed to avoid limitations concerning the global availability of oxygen. The amount of oxygen necessary to completely oxidize GLY to carbon dioxide and water (200 mL, 0.3 M) at 60 °C would be less than 12 mL at a pressure of 50 bar, which meant that using our test rig equipped with a 300 mL oxygen reserve initially pressurized at 50 bar, we would consume much less than 6 vol% of oxygen. Thus, under our conditions, the observation of a dependency of conversion on the partial pressure of oxygen would stem from limitations placed by oxygen dissolution rates (i.e., in a diffusional regime). To confirm that we worked in a chemical regime, a series of experiments under an oxygen pressure of 2.8, 5, and 10 bar were carried out.

Figure 8 shows that the differences between GLY transformations at various oxygen pressures are negligible in both kinds of tests (gold-catalyzed and base-induced). For example, after 60 and 100 min of a reaction with Au nanoparticles under an oxygen atmosphere at a pressure of 2.8, 5 and 10 bar, GLY conversions were in the range of 19–22 % after 60 min and 33–37 % after 100 min, respectively (Figure 8 b), which corresponded to an absolute difference lower than 4 % in any case. For the base-induced transformation, the differences were even smaller, as GLY conversion was in the range of 4.8–5 % after 60 min and 9–10 % after 100 min (Figure 8 a).

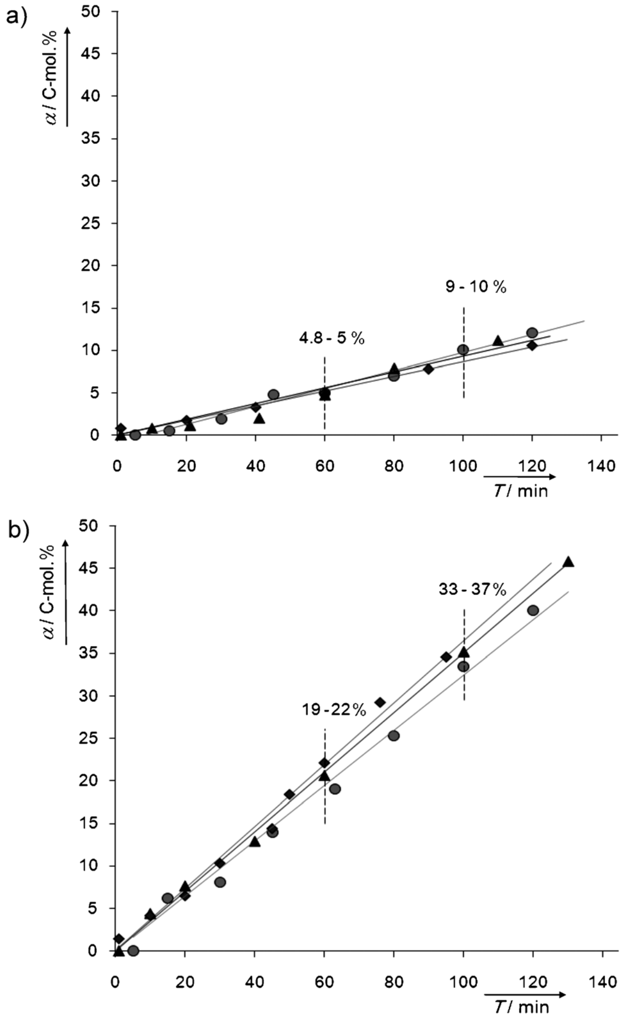

Figure 8. Comparison of GLY conversion a) in the absence (blank tests) and b) in the presence of the gold catalyst under variable O_2 pressure [2.8 (●), 5 (◆), and 10 bar (▲)]. Reaction conditions: aq. GLY (0.3 M), 60 °C, NaOH/GLY = 4 (molar ratio), GLY/Au molar ratio equal to ∞ for blank tests or 3500 for catalytic tests.

Effect of reaction temperature

Another important parameter was reaction temperature. Thus, a series of catalytic and noncatalytic tests with analogous concentrations of GLY and base were performed. All tests performed in the absence of the gold catalyst prove that at higher temperatures and in the presence of oxygen and base, GLY is mainly oxidized to glycolic and formic acid, whereas glyceric acid production is less favored (Figure 9). Above 80 °C, small amounts of tartronic and oxalic acid were also detected with maximum yields of 1 and 0.2 %, respectively, after 3 h at 80 °C (Figure 9 f) and twice larger at 100 °C (Figure 9 h). A significantly different product distribution was observed in tests in the presence of gold, in which glyceric acid was the main product ($>$50 %) up to 80 °C. Moreover, at lower temperatures (40–60 °C) the yield of formic acid was higher than that of glycolic acid, whereas at higher temperatures the opposite trend was observed. Nevertheless, in blank tests, the selectivity sequence remained unchanged with temperature. Thus, for catalytic tests at 100 °C, increased decomposition of GLY to lower molecules, (glycolic and formic acid) influenced product distribution.

Notably, GLY decomposition is characteristic of blank tests. All these observations can put forward the assumption that during the liquid-phase oxidation reaction, GLY transformation can follow two different reaction pathways. However, because through both pathways (the gold-catalyzed oxidation and the conversion process induced by the presence of a base) the main products remain the same, it seems that these two processes (consisting of sequences of simultaneous reactions) occur in parallel. The main difference in catalytic and noncatalytic tests exclusively stems from the proportion (balance) between the relative contribution of both pathways (i.e., some reactions are favored in the presence of the gold catalyst and others in its absence). To confirm such an assumption, the apparent activation energies (E_a) for both reaction modes were calculated from the initial rate values of GLY conversion at different temperatures. As we can see in Figure 10, the E_a calculated from the Arrhenius plot for gold-catalyzed reactions is much smaller than that of the base-induced transformation, with respective values of 61.4 and 93.5 kJ mol^{-1}.

Additionally, the good linearity of Arrhenius plots and the range of calculated apparent activation energies are in excellent agreement with the assumption of a chemical regime.

These results also give an idea about the stability of the catalyst at elevated temperatures ($\geq$80 °C). Indeed, if gold nanoparticles were insufficiently protected, we would obtain consid-

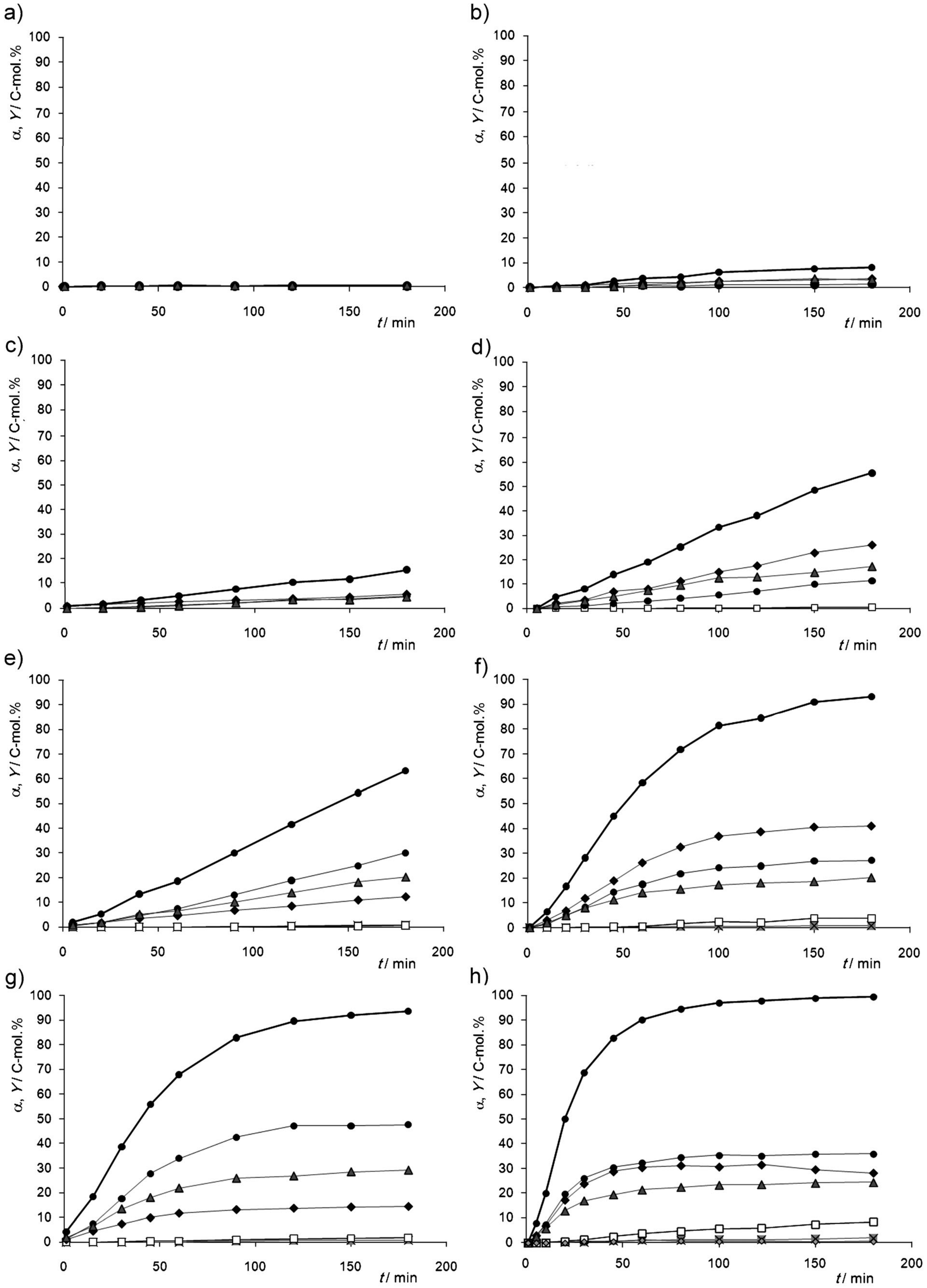

Figure 9. Comparison of GLY conversions (●) and yields of the main products [oxalic (☒), tartronic (□), glyceric (◆), glycolic (●), formic (▲), and acetic acid (◆)] obtained for blank tests (left) with the results of GLY oxidation in the presence of gold nanoparticles (right) at 40 (a, b), 60 (c, d), 80 (e, f), and 100 °C (g, h). Reaction conditions: aq. GLY (200 mL, 0.3 M), NaOH/GLY = 4 (molar ratio), GLY/Au molar ratio equal to ∞ (blank tests) or 3500 (catalytic tests), oxygen pressure: 5 bar.

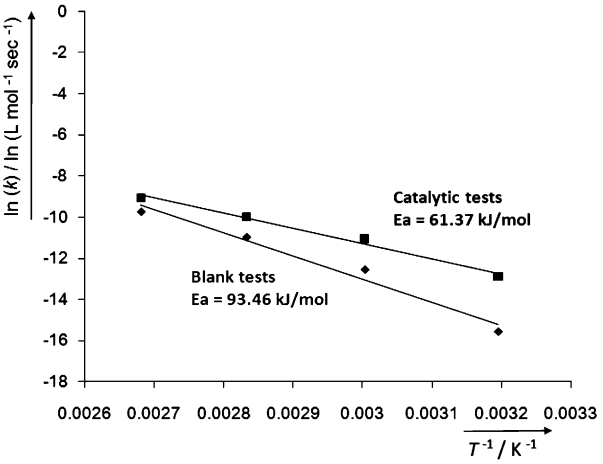

Figure 10. Arrhenius plots for gold-catalyzed and base-induced GLY transformations (calculations performed on the basis of initial reaction rates, determined from data in Figure 9).

erably less different results in the presence and absence of gold nanoparticles.

Systematic critical analysis of possible reaction pathways

By systematically analyzing the literature and the reaction schemes proposed for the liquid phase oxidation of GLY we can appreciate the complexity of the process, especially when a gold catalyst and a base are used at the same time.[1,9,22,26–29] Separation of the metal-catalyzed reactions from the noncatalytic transformation of GLY in the liquid phase under basic conditions is even more difficult because there is a lack of information in the literature. Subsequently, we mainly concentrated on the noncatalytic conversion of GLY and its derivatives under basic conditions. The cited literature was supported by appropriate theoretical calculation data and experimental results, which led to the proposal of a final global reaction scheme.

GLY activation and initial transformation in the presence of base only

The amount of GLY converted at temperatures above 80 °C after 3 h of reaction in the absence of a catalyst was really surprising, especially because it is hard to find similar experiments (without gold or other metallic catalyst and in the presence of a base alone) in the literature. The only information we found is in the work of Kwon et al.,[30] in which the authors underlined that alcohols with low pK_a values, such as GLY, have a high oxidation activity at $pH \geq 11$ in the presence of molecular oxygen. Under such reaction conditions, the alcohol is deprotonated to the corresponding alkoxide [Eq. (2)], which is thought to be more reactive in oxidation reactions than alcohol and acts as an aldehyde precursor [Eq. (3)].

$$H_\beta R{-}OH_\alpha \rightleftharpoons H_\beta R{-}O^- + H_\alpha^+ \tag{2}$$

$$H_\beta R{-}O^- \rightarrow R{=}O + H_\beta^+ + 2\,e^- \tag{3}$$

The first step is base-induced with no essential role for the metal catalyst.[30–32] Nevertheless, it is generally accepted that Equation (3) possibly involves a catalytic interaction with surface-bound hydroxide, which facilitates the resulting glyceraldehyde (GLAD) to be transformed to glyceric acid. Such a “surface-catalyzed” process is expressed by Equations (4) and (5).[10,33]

$$RCH_2OH_{ads} \rightarrow RCHO_{ads} + 2\,H_{ads} + 2\,e^- \tag{4}$$

$$RCHO_{ads} + H_2O \rightarrow RCOOH_{ads} + 2\,H_{ads} + 2\,e^- \tag{5}$$

However, Zope et al.[32] stated that both solution-mediated and metal-catalyzed steps must be involved in alcohol oxidation to acid at a high pH, which is usually seen as the most reasonable option. Additionally, Kwon et al.[30] proved that OH^- in solution can be more important for the overall reactivity than OH bound to the gold catalyst.

The possibility of GLY activation and transformation in the presence of a base alone was also confirmed by our blank tests in both the glass (Figure 3 a) and the stainless steel reactor (Figures 3 b and 4–9), in which GLY was oxidized in the absence of a gold catalyst. However, it is known from the literature that even traces of transition metals can induce GLY oxidation (especially in basic environments).[34] To exclude such a possibility and thus be absolutely sure that these unexpected results are not artifacts, we carefully carried out an additional test, in which the strictest precautions were taken using ultrapure reagents and exclusively nonmetallic equipment including a nonmetallic reactor.

Results of additional tests with ultrapure reagents in a specific nonmetallic reaction device

In contrast to previous tests carried out in the glass reactor, in which both the air supplier and stirrer were made from stainless steel to provide high pressure and perfect mixing (at 1500 rpm), respectively, in this additional experiment we used a three-neck flask immersed in bath oil (80 °C), a new previously unused Teflon magnetic stirring bar for mixing (400 rpm), and a thin glass tube for introducing oxygen at a flow rate of 50 mL min^{-1} directly to the agitated reaction mixture (Figure 11). HPLC-grade water instead of distilled water and a NaOH solution of high purity (typically used in the domain of molecular biology) instead of reagent-grade NaOH were used. The reaction volume, component concentrations, and base/GLY ratio were kept the same as in conventional tests in the stainless-steal reactor.

GLY was oxidized even in such “sterile” conditions (Figure 12). Conversion was much lower relative to our previous tests, which can be explained by the lower oxygen concentration in the reaction mixture. However, even when using typical reagents with the same equipment, temperature, and reagent ratios, identical results (with regard to GLY conversion) were obtained (Figure 12, dotted line). This result confirmed the reliability of our previous blank tests in the more sophisticated reaction device.

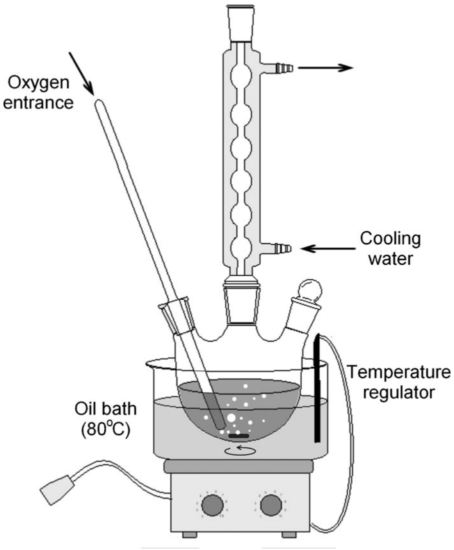

Figure 11. Apparatus used for reference test of GLY oxidation in the liquid phase with ultrapure reagents and nonmetallic equipment.

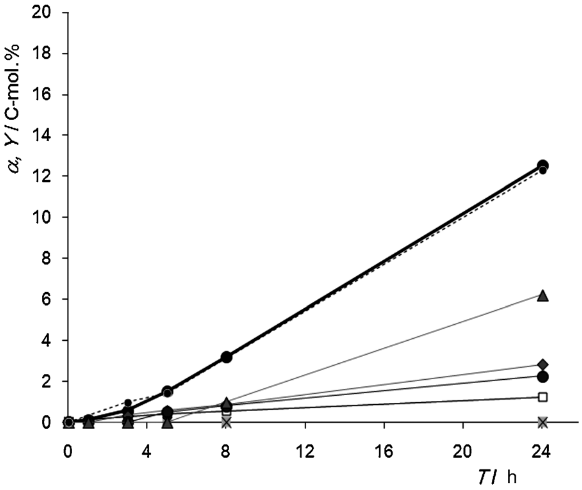

Figure 12. Comparison of GLY conversions (●) and yields of the main products [oxalic (☒), tartronic (□), glyceric (◆), glycolic (●), and formic acid (▲)] obtained for blank test carried out in the full glass reaction device with commercially available reagents of high purity. Reaction conditions: aq. GLY (200 mL, 0.3 M), NaOH/GLY = 4 (molar ratio), oxygen flow rate: 50 mL min^{-1}, 400 rpm, 80 °C, atmospheric pressure. Dotted line refers to GLY conversion under the same conditions but using standard reagents.

To further support our experimental results, theoretical calculations were performed, which confirmed the possibility of GLY transformation in the absence of a metal catalyst.

Results of theoretical calculations: Elimination pathway

From a theoretical point of view, various reaction mechanisms can be proposed for GLY activation in the absence of metallic nanoparticles. Due to the low pK_a of GLY, the equilibrium in Equation (2) is slightly shifted in favor of the alkoxide. However, when considering the subsequent GLY oxidation, the addition of a nucleophilic oxygen species on a negatively charged molecule may not be favored. Alternatively, strong basic media can favor elimination reactions. On an activated GLY molecule (according to the transition state represented in Figure 13) elimination of an OH moiety gives an enol, which is transformed into a ketone or an aldehyde by tautomerization. The unsaturated molecule can be oxidized by oxygen to give glyceric acid.

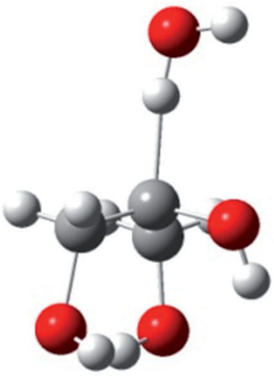

Figure 13. Transition state for the elimination reaction catalyzed by an OH$^-$ group. Grey: carbon; red: oxygen; white: hydrogen.

To confirm that this reaction is possible under the actual experimental conditions, we performed DFT calculations (B3LYP) taking into account the solvent (water) in the polarized continuum model (PCM) approximation. Two different C–H bonds may be broken (terminal or central) leading to 2-hydroxypropanal or 1-hydroxypropan-2-one (acetol), respectively (Scheme 1).

Both reactions are exothermic due to the formation of an enolate in a basic solution, but the abstraction of the central proton is favored. The computed activation energy is 77 kJ mol^{-1}. This value is slightly lower than the experimental one (93.5 kJ mol^{-1}; Figure 10), but this clearly indicates that the elimination mechanism must be taken into account in the absence of nanoparticles.

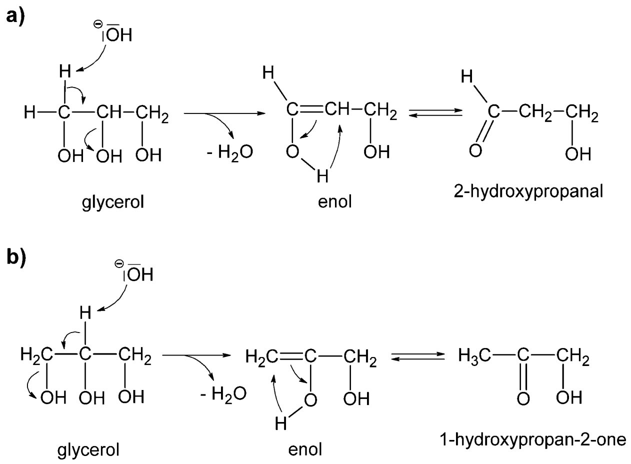

Scheme 1. Initial transformation of GLY, which is attacked by the base and, subsequently, the breaking of the a) terminal or b) central C–H bond occurs.

GLY oxidation through the noncatalytic radical pathway

Another pathway of GLY oxidation in the absence of metallic catalyst is related to the radical mechanism. This concept is based on the fact that the electrons released in Equation (3) can be accepted by molecular oxygen giving anion radicals [Eq. (6)]. Then, these can react with protons yielding hydrogen peroxide radicals [Eq. (7)].[35]

$$O_2 + e^- \rightleftharpoons O_2^{-\bullet} \quad (6)$$

$$O_2^{-\bullet} + H^+ \rightleftharpoons {}^\bullet OOH \quad (7)$$

Subsequent steps can be expressed by free radical chain reactions, well-known from classical organic chemistry [Eqs. (8)–(11)].

$${}^\bullet OOH + RH \rightarrow H_2O_2 + R^\bullet \quad (8)$$

$$H_2O_2 \rightarrow 2\,{}^\bullet OH \quad (9)$$

$$R^\bullet + O_2 \rightarrow ROO^\bullet \quad (10)$$

$$ROO^\bullet + RH \rightarrow ROOH + R^\bullet \quad (11)$$

Commonly, free radical reactions proceed at elevated temperatures in the gas phase. However, according to Denisov and Afanas'ev,[35] alcohols can undergo self-oxidation, in which free radicals are formed by bimolecular and trimolecular reactions involving the alcohol and dioxygen [Eq. (12) and (13), respectively].

$$HROH + O_2 \rightarrow HOR^\bullet + {}^\bullet OOH \quad (12)$$

$$2\,HROH + O_2 \rightarrow HOR^\bullet + H_2O_2 + R^{\cdot} \quad (13)$$

The same arguments are also made by Bamford and Tipper,[36] who claim that such reactions can occur in the liquid phase under moderate temperatures (up to 100 °C) even in the absence of initiators.

It is worth adding that the formation of hydrogen peroxide and the dissociation of peroxide and hydrogen peroxide intermediates are also regarded as possible ways of oxygen activation in catalytic liquid-phase oxidation reactions.[32,33] Further steps of oxidation on the catalyst surface are well-established in the literature.[25,32,33] However, such steps can also proceed through a noncatalytic radical pathway. For example, we can refer to the results reported previously by Andronov et al.,[37,38] who studied the possibility of GLAD oxidation in an aqueous solution in the presence of only oxygen and a base. That reaction proceeded through a chain mechanism leading to CO_2, glyceric, glycolic, acetic, and formic acid as final oxidation products, with glycolic aldehyde and methylglyoxal as intermediates. The proposed reaction scheme included the formation of $RO_2^{\cdot}$, that is, the (2,3-dihydroxypropyl)dioxidanyl radical, which subsequently reacted with another molecule giving another radical and hydroperoxide, which easily converted to glyceric acid (Scheme 2).

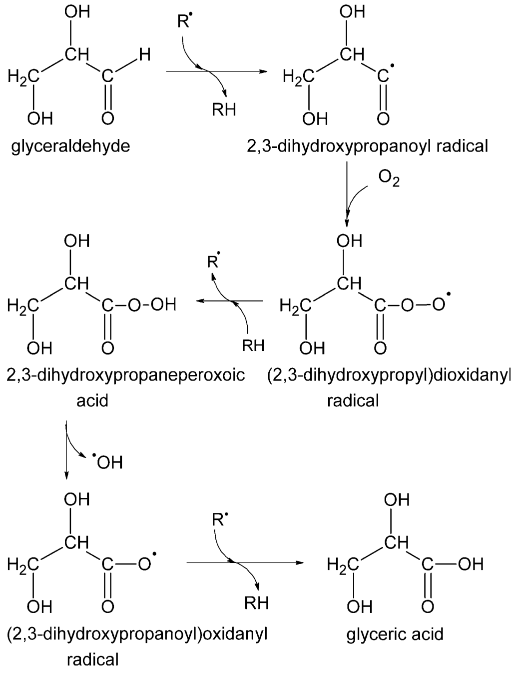

Scheme 2. Possible mechanism of radical chain reactions from GLAD to glyceric acid (adapted from Ref. [37&38]). GLAD was not detected in our conditions.

However, peroxide radicals can undergo further isomerization reactions followed by cleavage of the C–C bond [Eq. (14)].

$$RO_2^\bullet \rightarrow R'CHO + R''O^\bullet \quad (14)$$

During such reactions, carbon dioxide should appear in measurable amounts. The most important assumption was that this type of reaction could proceed both in a heterogeneous and a homogenous fashion, (on the catalyst surface or in solution).[37]

Notably, the main products in our catalytic tests were always glyceric, glycolic, and formic acid, whereas CO_2, GLAD, and dihydroxyacetone (DHA) did not appear in significant amounts (no pressure increase during the process, carbon balances in the range of 95–100 %, no HPLC signal, and also negative result of the Trommer probe for aldehydes). Nevertheless, because GLAD is the first and main intermediate that is mentioned in the literature for the GLY liquid-phase partial oxidation reaction,[1] we should take into account the possibility of its existence as an intermediate, rapidly consumed in subsequent reactions.

Kinetic experiments performed by Andronov et al.[37] for GLAD proved that alkaline hydrolysis was induced by the presence of high amounts of base, because above pH 8 the rate of accumulation of acids increased sharply. It was concluded that the rate of such reactions was superimposed upon the rate of oxidation with a radical character. That means that for high NaOH concentrations, the yield in glycolic and formic acid should be larger than the yield in glyceric acid. Especially glycolic acid should dominate in the reaction mixture because it can also be formed through radical splitting with carbon dioxide formation. Similar reactions should also be observed during GLY oxidation in highly basic solutions. Temperature variation showed that such a situation occurs only in noncatalytic processes (Figure 9). In the presence of gold nanoparticles, glyceric acid was the most important product and only at high temperatures (above 80 °C) its yield slightly decreased to the benefit of tartronic acid (Figure 9 h). Similarly, Porta and Prati[23] proved that increasing the temperature promoted the oxidation of glyceric acid to tartronic acid. Moreover, in the presence of carbon-supported gold catalysts glyceric acid was the main product and high amounts of base could even further promote its formation. The same relationship between temperature, amount of base, and generation of glyceric and tartronic acid was also observed by Sakurai et al.[11] for gold nanoclusters stabilized by poly(1-vinylpyrrolidin-2-one) (PVP). After 24 h of oxidation in open air at 80 °C in aqueous NaOH, a GLY conversion of 94 % was obtained with a selectivity towards tartronic, glyceric, and glycolic acid of 32, 24, and 11 %, respectively. Surprisingly, these authors did not observe any formation of formic acid. Nevertheless, we have to point out that they used a large excess of gold (GLY/Au molar ratio was calculated to be 200), which normally should favor deep oxidation reactions to carbon dioxide, and also to tartronic and oxalic acid. The same effect should be also caused by using gold nanoparticles of a small diameter,[1,16,39] that is, Au–PVP with an average size of (1.3 ± 0.3) nm. On the other hand, not only the selectivity but mostly the overall activity strongly depended on the size of gold particles.[1,16] Moreover, the type of protecting agent used for gold nanoparticle synthesis can also influence the final results (in our case, protection was supplied by sodium citrate, which is able to surround gold particles preventing their agglomeration).

Possible formation mechanisms of C_2 and C_1 derivatives

From experimental results (Figures 3–9) we concluded that the formation of small molecules (glycolic and formic acid) gains in significance especially at high temperatures and in the absence of a gold catalyst. In such conditions, the reaction pathway through the alkaline C–C bond cleavage seems to be the most probable one (Scheme 3). In this mechanism, glycolic and formic acid can be directly formed from GLAD or glyceric acid. It is an example of a retro-aldol reaction.[40] Usually, this reaction is less favorable than classical condensation, in which an additional irreversible step of β-hydroxyaldehyde dehydration appears.[40,41]

An analogous reaction can be also assumed for hydroxypyruvic acid, which is another GLY derivative, (Scheme 4). In this case, glyoxylic acid and formaldehyde are the main products, which can undergo subsequent transformation to glycolic and formic acid through a Cannizzaro cross-reaction (Scheme 5). All these reactions proceed in the presence of a base without CO_2 formation.

The occurrence of the C–C bond cleavage in aqueous basic solutions was previously mentioned by Dimitratos et al.[42] and Porta and Prati[23] for GLY oxidations over gold–palladium nanocrystals and carbon-supported gold catalysts, respectively, and also by Andronov et al.[37] for GLAD oxidations. Additionally, for hydroxypyruvic acid it is possible to envisage another mechanism for C–C bond breaking, analogous to the well-known transformations of sugars in basic media.[43]

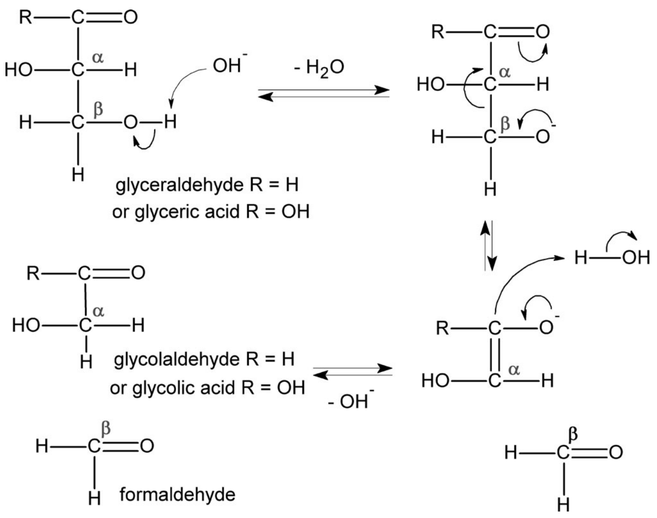

Scheme 3. Possible mechanism of the retro-aldol reaction for GLAD and glyceric acid in the presence of a base.

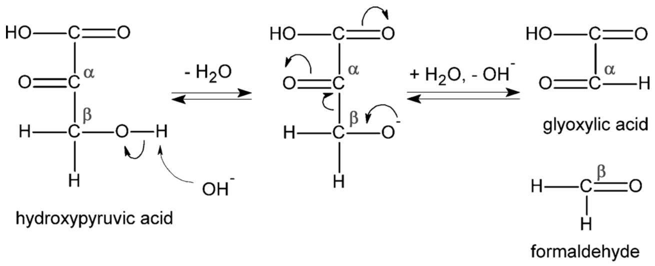

Scheme 4. Possible mechanism of C–C bond cleavage in hydroxypyruvic acid.

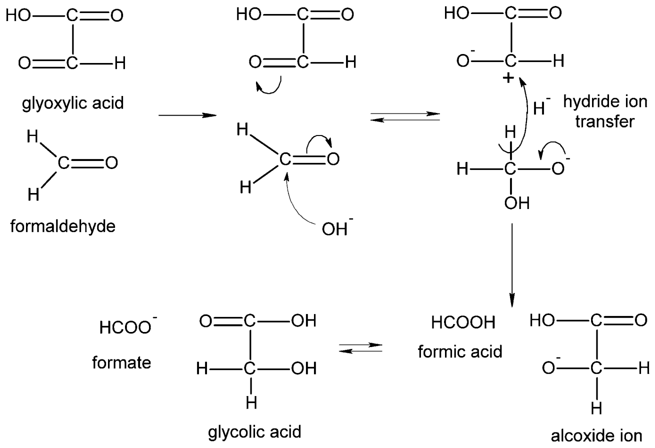

Scheme 5. Mechanism of the Cannizzaro cross-reaction for glyoxylic acid and formaldehyde.

In the hydrolytic α- and β-dicarbonyl cleavage of hydroxypyruvic acid and its isomer 2-hydroxy-3-oxo-propanoic acid, respectively, formic and glycolic acid are generated in equal amounts (Scheme 6). Generally, it can be assumed that low molecular weight hydroxyacids arise from corresponding hydroxycarbonyls and α-dicarbonyls by direct oxidation and intermolecular Cannizzaro reactions, respectively.

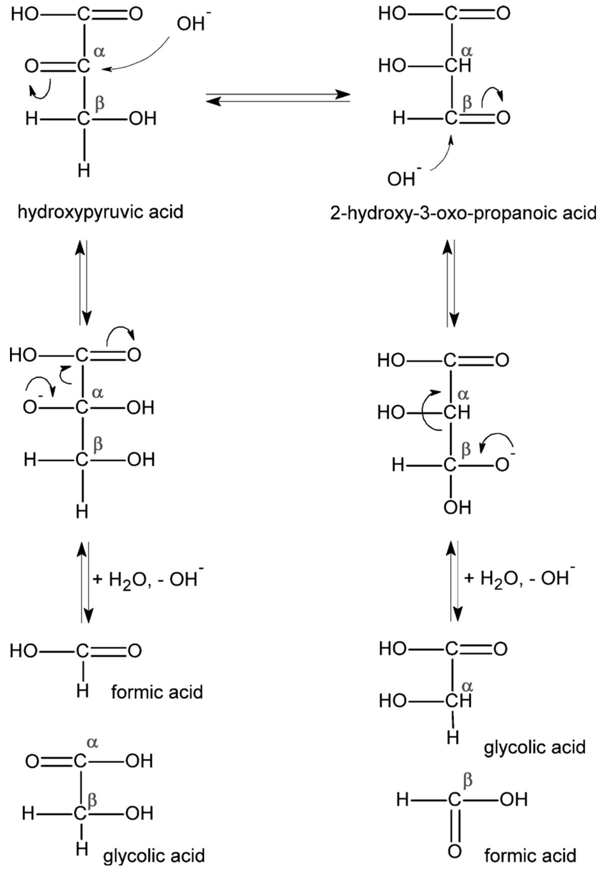

Scheme 6. Possible mechanism of α- and β-dicarbonyl cleavage.

The problem of aldehydes in the reaction mixture

In all GLY oxidation tests under our reaction conditions (temperatures of 40–100 °C, O_2 at a pressure of 2.8–5 bar, mixing speed equal to 1500 rpm, NaOH/GLY molar ratio of up to 4, and a Turkevich Au concentration of 0–0.146 mmol L^{-1}) we never detected any aldehyde (no HPLC signal and negative results of the Trommer probe with Cu^{2+}). Thus, we could conclude that under our conditions these compounds could be treated as unstable intermediates, immediately converted to the corresponding acids. This was confirmed by an additional test with a pure GLAD solution (0.1 M), which, after addition of a base at room temperature and even in the absence of oxygen and catalyst, was easily transformed to a number of derivatives. Moreover, its structural isomer (tautomer) DHA behaved in the same way. Oxidation of these compounds (GLAD and DHA) in the presence of a gold catalyst gave glyceric, glycolic, and formic acid, together with a complex mixture of various derivatives, which were never observed during conventional GLY oxidation tests (Figure 14).

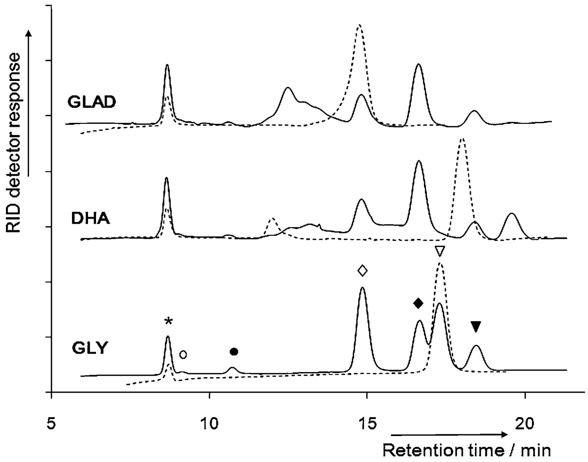

Figure 14. Comparison of typical chromatograms recorded after 60 min of reaction of GLAD (0.1 M), DHA (0.1 M), or GLY (0.3 M) in standard conditions (60 °C, oxygen pressure: 5 bar, propeller speed: 1500 rpm, 9.6 g NaOH, and 86 μM of commercial gold catalyst). Each dotted line corresponds to an initial reaction mixture. The marks represent: sulfuric acid (*) used for the dilution of samples before HPLC analyses, oxalic acid (○), tartronic acid (●), glyceric acid (◇), glycolic acid (◆), GLY (▽), and formic acid (▼).

Moreover, in each test after 15–20 min the Trommer probe produced a negative result, meaning (together with HPLC analyses) that, under our typical process conditions, the conversion of both DHA and GLAD was complete in a short time.

Glyoxylic acid and formaldehyde were other examples of two aldehydes, which in theory could appear in the reaction mixture, but were not detected under our conditions. Although the Cannizzaro reaction can explain this absence, an additional test was carried out to confirm this assumption. Using reaction conditions analogous to those used in the case of GLAD and DHA (aqueous solution of glyoxylic acid with a concentration of 0.1 M, 60 °C, O_2 at a pressure of 5 bar, propeller speed of 1500 rpm, Au with a concentration of 86 μM, and 9.6 g of NaOH), glyoxylic acid could be easily oxidized to oxalic acid (Figure 15). The same test was performed for an equimolar solution of glyoxylic acid and formaldehyde, which gave rise after 5 min oxalic, glycolic, and formic acid as the only products. After 20 min, the peak attributed to formaldehyde completely disappeared (Figure 15, solid line), whereas glyoxylic acid was still present in the reaction mixture. That meant that the oxidation of formaldehyde to formic acid proceeded more easily than the oxidation of glyoxylic acid to glycolic acid. Moreover, straight oxidation competed with the Cannizzaro reaction.

Discussion about the global integrated reaction scheme

Taking all the above observations into account and especially the absence of the majority of the possible byproducts, characteristic for GLAD and DHA oxidation in basic media (Figure 14), we can conclude that under our reaction conditions the possible global reaction pathway in the presence of Turkevich Au particles seems to be much simpler than the general combined one.[1]

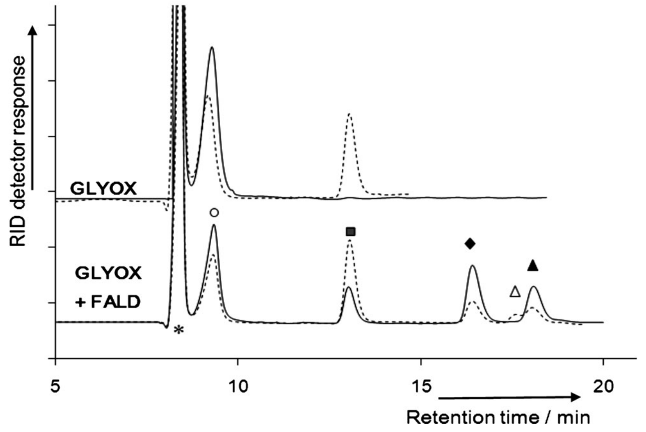

Figure 15. Comparison of typical chromatograms of glyoxylic acid (GLYOX, 0.1 M) and its equimolar mixture with formaldehyde (GLYOX + FALD) recorded after 5 (– – –) and 20 min (——) of reaction in standard conditions (same as those described in Figure 14). The marks represent: sulfuric acid (*), oxalic acid (○), glycolic acid (◆), glyoxylic acid (■), formaldehyde (△), and formic acid (▲).

Our proposed mechanism (Scheme 7) is based on experimental results of GLY oxidations in the presence of a base, and in both the presence and absence of a gold catalyst. Also, the results of short oxidation tests of all mentioned products (solutions with a concentration of 0.1 M in standard reaction conditions) were used to complete this global reaction scheme. Unfortunately, the lack of pure commercially available glyceric acid made it impossible to perform a test with this component. Such a test would have undoubtedly provided valuable information about the intermediate steps of the GLY oxidation process. Commercially available calcium salts of glyceric acid exhibited an unusual behavior, because they had low solubility in water and formed basic solutions. Moreover, we believe that the introduction of calcium cations into the reaction mixture would have influenced oxidation results.

There are two main possible pathways for the primary GLY transformation (Scheme 7). First, GLY is directly oxidized to glyceric acid, because the observed selectivity at the initial stages of each process is the highest, and especially at lower temperatures it approximates 100 % (possibility of GLAD formation as discussed above). This reaction proceeds favorably in the presence of a catalyst, a base, and an excess of oxygen (Scheme 7, CR++, NCR+). The second possible primary transformation is a direct oxidative cleavage, in which glycolic and formic acid are directly formed from GLY, probably through the formation of highly reactive radical-type species without intermediate formation of partially oxidized C_3 products (e.g., glyceric acid). This reaction requires the presence of a base and oxygen, whereas the presence of a catalyst seems not to be mandatory. This possibility is suggested by previous research concerning propanediol conversion (oxidative cleavage) in the gas phase in the absence of a catalyst.[44] Furthermore, this hypothesis is supported by preliminary kinetic modeling work (not shown here), which suggests that taking into account the direct oxidative cleavage is mandatory to correctly fit experimental data to the theoretical model. Thus, we cannot exclude further oxidative cleavage of glycolic acid towards oxidized C_1 products.

Notably, in the absence of oxygen GLY conversion is almost completely suppressed. Even when using a base and operating at the relatively high temperature of 80 °C, the conversion of GLY after 1 h under a N_2 atmosphere, in the absence of oxygen and without the gold catalyst, hardly exceeded 0.5 %. This also confirms that the initial C–C splitting of GLY (the second possible primary transformation, Scheme 7) demands the assistance of oxygen. Then, glyceric acid can be split into glycolic acid and C_1 components (Scheme 3), mainly formaldehyde (Scheme 7, NCR++, CR+). The latter is supposedly immediately oxidized to formic acid by oxygen (Scheme 7, CR++) or is involved in the sequence of Cannizzaro-type cross-reactions (Scheme 5). The results of blank tests (Figure 8) suggest that these reactions can be favored especially at higher temperatures and in the absence of a gold catalyst (Scheme 7, NCR++). Further oxidation of glyceric acid to tartronic acid seems to proceed through the formation of hydroxypyruvic acid (Scheme 7, CR++), which can easily undergo classical hy-

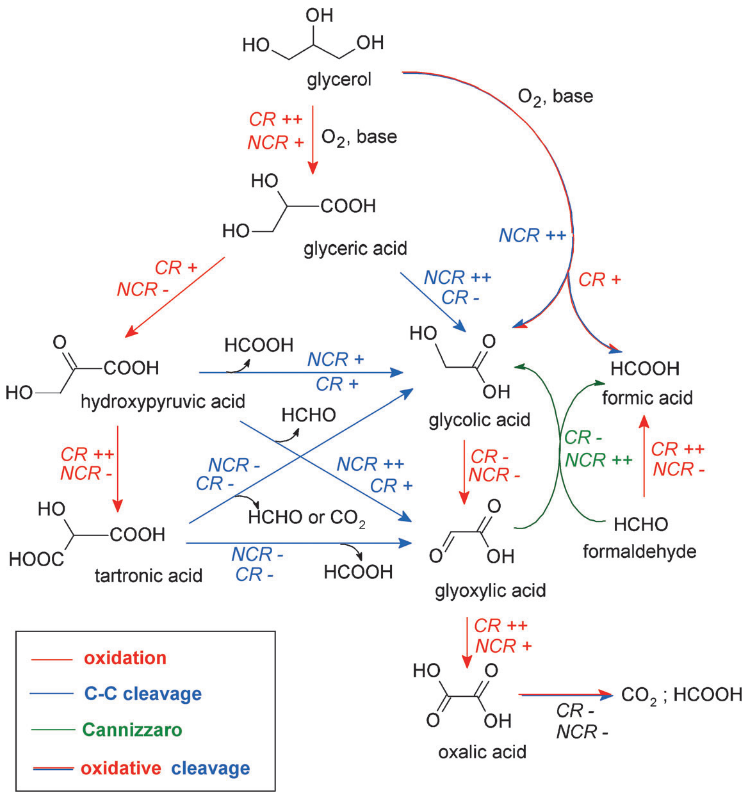

Scheme 7. Possible pathways for GLY oxidation with and without gold nanoparticles. Red, blue, and green arrows correspond to simple oxidation, C–C cleavage reactions, and Cannizzaro reactions, respectively. Abbreviations CR and NCR stand for catalytic and noncatalytic reaction, respectively, whereas the number of "+" and "–" after CR and NCR signifies the extent to which each reaction is favorable (relative preponderance of each reaction to assess its contribution to the observed product distribution).

drolytic C–C cleavage (Scheme 7, NCR++), as well as a variety of subsequent reactions (Schemes 3–5). The last possible products (i.e., glyoxylic and oxalic acids) can be generated by direct oxidation and/or oxidative cleavage reactions from both tartronic and glyceric acid. It seems that direct oxidation is favored in the presence of gold nanoparticles, whereas high temperatures and strong basic conditions favor oxidative cleavage and straight hydrolytic transformations, such as: retro-aldol (Scheme 3), α- and β-dicarbonyl cleavage (Scheme 6), oxidative cleavage with carbon dioxide evolution, and Cannizzaro cross-reactions (Scheme 5).

Experimental Section

Reagents

All chemicals were used as received without any further purification. For the preparation of colloidal gold nanoparticles the following reagents were used: $HAuCl_4$ (99.99 %) from Alfa Aesar; $Na_3C_6H_5O_7$ (99 %) from Sigma–Aldrich. For the catalytic tests, anhydrous GLY (99 %) and pure NaOH from Sigma–Aldrich were used. All solutions were prepared with distilled water (Autostill 4000x filter system). The eluent used for chromatographic analyses was prepared from HPLC-grade solvents: H_2SO_4 (0.25 M) from Fluka, deionized water, and CH_3CN from Sigma–Aldrich.

Preparation of gold nanoparticles

The preparation of the gold colloid was performed according to the original procedure reported by Turkevich et al.[45,46] In a typical preparation, distilled water (212.5 mL) was heated with vigorous stirring under reflux. Then an aqueous solution of $HAuCl_4$ (25 mL, 5.4 mM) was added to boiling water and the resulting solution was kept under mechanical stirring until boiling was reached again. Then an aqueous solution of sodium citrate (12.5 mL, 10 mg mL^{-1}) was added. The system was then kept under reflux for 30 min. During the procedure, the flask was covered with aluminum foil to prevent any exposure to the sunlight, which could accidentally initiate the reduction of the gold precursor ($HAuCl_4$). Finally, the resulting colloid solution was cooled by a "fast-quenching process", by dipping the flask in a cold water bath (5 °C).

Characterization of gold nanoparticles

The characterization of gold samples did not involve any filtration or centrifugation processes. UV/Vis spectra of gold nanoparticle solutions were measured by using a PerkinElmer Lambda 650S spectrophotometer. For TEM measurements, a drop of each synthesized Au solution was deposited on a copper-coated grid, which was subsequently dried for 5 h before being examined by means of a TEM FEI Tecnai G2-20 twin with an accelerating potential of 200 KV.

GLY oxidation tests

Typical experiments were carried out in a 300 mL semibatch stainless steel reactor equipped with a gas-induced turbine, four baffles, a thermocouple, a thermoregulated oxygen supply system, and a pH electrode. In each experiment, a solution of GLY and gold in water (200 mL) was heated to the desired temperature (40–100 °C), and the reaction was started when the calculated amount of sodium hydroxide was flushed into the reactor through a specific fast-introduction device and the system was pressurized (2.5–10 bar) under continuous stirring (1500 rpm). In all experiments, the initial concentration of GLY was equal to 0.3 M, whereas the amount of base was adjusted to give a NaOH/GLY molar ratio between 0 and 4. In most experiments, the GLY/gold molar ratio was fixed to 3500. The temperature, pH, and O_2 pressure were continuously monitored and the reaction mixture was periodically analyzed by means of an Agilent 1200 HPLC equipped with a Rezex ROA-Organic Acid H^+ column (300 × 7.8 mm) and a reflective index detector. A solution of H_2SO_4 (2.4 mM) and CH_3CN (0.1 mM) in deionized water (0.48 mL min^{-1}) was used as eluent. Before analysis, the samples were diluted and acidified to quench the reaction, whereas the identification and quantification of products was achieved by comparison with calibration curves.

Trommer probe for aldehydes

The Trommer probe was used to detect the presence of aldehydes (GLAD, formaldehyde, or glycolaldehyde) in the reaction mixture using the reaction in Equation (3). Moreover, because of the possibility of tautomeric keto–aldol transformation in the basic solution, this test could also indirectly indicate the presence of components such as DHA. All these components could reduce the bright blue Cu^{2+} ions to red Cu^+ ions.

$$2\,\mathrm{Cu(OH)_2} + \mathrm{RCHO} + \mathrm{OH^-} \rightarrow \mathrm{Cu_2O} + \mathrm{RCOO^-} + 3\,\mathrm{H_2O} \tag{3}$$

Typically, a reaction-mixture sample (0.5 mL) was added to a freshly prepared colloidal $Cu(OH)_2$ solution (0.5 mL), which was produced by adding 2–3 droplets of aqueous sodium hydroxide (1 M) to an aqueous copper sulfate solution (0.1 M). Color changes were observed after 5 min at RT.

DFT calculations

DFT calculations (Table 1) were performed using the G03 program.[47] For both gas phase and liquid phase, we used B3LYP[48] approximations to compute the electronic energy. The core electrons were described by a pseudopotential,[49] whereas double-zeta basis sets were used for the valence one. The solvent was described by the PCM model.[50] A polarization sphere was added on the H involved in the reaction.

All geometries were fully optimized without constraint, and frequency calculations were performed to characterize transition states and stable geometries. The C–H bond distance in the transition state was very large (1.5 Å). The reaction mechanism corresponded in the same step to the C–H and C–OH bonds breaking, which explained the very long C–H distance. The departure of the OH^- group was favored by the formation of an enolate and the transfer of a proton to the leaving group. The presence of three OH groups on the molecule was the key to the peculiar GLY behavior because they increased the low acidity of the C–H bond by an inductive effect and stabilized the leaving group by proton

Table 1. Calculated activation energies and C–H, C–OH bond distances.

Reaction	E_a [kJ mol^{-1}]	Bond distances [Å] C–H	C–OH
ketone formation	gas phase: 42	1.78	1.67
ketone formation	liquid phase: 77	1.88	1.63
aldehyde formation	gas phase: 58	1.61	1.51

transfers. The activation-energy difference between the two possible sites was large. We proposed that the reaction would only produce ketones.

Notably, the activation-energy variation between the gas phase and the liquid phase was due to the screening of the bare charge by the solvent.

Acknowledgements

For the financial support, the authors would like to thank the European Union through the European Social Fund within the Cracow University of Technology development program—top quality teaching for the prospective Polish engineers; University of the 21st century project (contract no.UDA-POKL.04.01.01-00-029/10-00). We would also like to thank Dr. Ahmed Addad (CNRS UMR 8207 - Université Lille 1 for TEM analyses of gold particles.

Keywords: density functional calculations · gold · heterogeneous catalysis · nanoparticles · oxidation

[1] B. Katryniok, H. Kimura, E. Skrzyńska, J.-S. Girardon, P. Fongarland, M. Capron, R. Ducoulombier, N. Mimura, S. Paul, F. Dumeignil, *Green Chem.* **2011**, *13*, 1960.
[2] M. Pagliaro, M. Rossi, *The Future of Glycerol: New Usages for a Versatile Raw Material*, Royal Society of Chemistry, **2008**.
[3] P. Gallezot, *Catal. Today* **2007**, *121*, 76.
[4] A. Behr, J. Eilting, K. Irawadi, J. Leschinski, F. Lindner, *Green Chem.* **2008**, *10*, 13.
[5] N. Rahmat, A. Z. Abdullah, A. R. Mohamed, *Renewable Sustainable Energy Rev.* **2010**, *14*, 987.
[6] B. Katryniok, S. Paul, V. Belliere-Baca, P. Rey, F. Dumeignil, *Green Chem.* **2010**, *12*, 2079.
[7] B. Katryniok, S. Paul, M. Capron, F. Dumeignil, *ChemSusChem* **2009**, *2*, 719.
[8] B. Katryniok, S. Paul, V. Belliere-Baca, P. Rey, F. Dumeignil, *Green Chem.* **2010**, *12*, 1922.
[9] L. Prati, P. Spontoni, A. Gaiassi, *Top. Catal.* **2009**, *52*, 288.
[10] M. Besson, P. Gallezot, *Catal. Today* **2000**, *57*, 127.
[11] Y. S. Salprima, R. N. Dhital, H. Sakurai, *Tetrahedron Lett.* **2011**, *52*, 2633.
[12] M. Comotti, C. Della Pina, R. Matarrese, M. Rossi, *Angew. Chem.* **2004**, *116*, 5936; *Angew. Chem. Int. Ed.* **2004**, *43*, 5812.
[13] P. Beltrame, M. Comotti, C. Della Pina, M. Rossi, *J. Catal.* **2004**, *228*, 282.
[14] P. G. N. Mertens, I. F. J. Vankelecom, P. A. Jacobs, D. E. De Vos, *Gold Bull.* **2005**, *38*, 157.
[15] P. Suramanee, S. Poompradub, R. Rojanathanes, P. Thamyongkit, *Catal. Lett.* **2011**, *141*, 1677.
[16] A. Villa, D. Wang, D. S. Su, L. Prati, *ChemCatChem* **2009**, *1*, 510.
[17] S. Basu Basu, G. Soumen, K. Sujit, S. Kundu, S. Panigrahi, S. Praharaj, S. Pande, S. Jana, T. Pal, *J. Colloid Interface Sci.* **2007**, *313*, 724.
[18] I. Ojea-Jiménez, F. M. Romero, N. G. Bastús, V. Puntes, *J. Phys. Chem. C* **2010**, *114*, 1800.
[19] W. Haiss, N. T. K. Thanh, J. Aveyard, D. G. Fernig, *Anal. Chem.* **2007**, *79*, 4215.
[20] A. Sobczak-Kupiec, D. M. Zimowska, Z. Wzorek, *Digest J. Nanomater. Biostructures* **2011**, *6*, 803.
[21] D. T. Nguyen, D.-J. Kim, M. G. So, K.-S. Kim, *Adv. Powder Technol.* **2010**, *21*, 111.
[22] S. Demirel-Gülen, M. Lucas, P. Claus, *Catal. Today* **2005**, *102–103*, 166.
[23] F. Porta, L. Prati, *J. Catal.* **2004**, *224*, 397.
[24] S. Carrettin, P. McMorn, P. Johnston, K. Griffin, G. J. Hutchings, *Chem. Commun.* **2002**, 696.
[25] P. Gallezot, *Catal. Today* **1997**, *37*, 405.
[26] S. Gil, M. Marchena, L. Sanchez-Silva, A. Romero, P. Sanchez, J. L. Valverde, *Chem. Eng. J.* **2011**, *178*, 423.
[27] N. Dimitratos, A. Villa, L. Prati, *Catal. Lett.* **2009**, *133*, 334.
[28] E. G. Rodrigues, S. A. C. Carabineiro, J. J. Delgado, X. Chen, M. F. R. Pereira, J. M. Órfão, *J. Catal.* **2012**, *285*, 83.
[29] A. Villa, A. Gaiassi, I. Rossetti, C. L. Bianchi, K. van Benthem, G. M. Veith, L. Prati, *J. Catal.* **2010**, *275*, 108.
[30] Y. Kwon, S. C. S. Lai, P. Rodriguez, M. T. M. Koper, *J. Am. Chem. Soc.* **2011**, *133*, 6914.
[31] A. Martin, M. P. Checinski, M. Ritcher, *Catal. Commun.* **2012**, *25*, 130–135.
[32] B. N. Zope, D. D. Hibbitts, M. Neurock, R. J. Davis, *Science* **2010**, *330*, 74.
[33] V. R. Gangwal, J. van der Schaaf, B. F. M. Kuster, J. C. Schouten, *J. Catal.* **2005**, *229*, 389.
[34] *Glycerine: An Overview.* The Soap and Detergent Association, Glycerine & Oleochemical Division, New York, **1990**. Available from: http://www.aciscience.org/Oleochemical/Glycerine.aspx.
[35] E. T. Denisov, I. B. Afanas'ev, *Oxidation and Antioxidants in Organic Chemistry and Biology.* Taylor&Francis Group, **2005**.
[36] C. H. Bamford, C. F. H. Tipper, *Liquid Phase Oxidation* (Comprehensive chemical kinetics. Section 6, Oxidation and combustion reaction, vol. 16), Elsevier Scientific Publishing Company, **1980**.
[37] L. M. Andronov, Z. K. Maizus, N. M. Emanuel, *Izv. Akad. Nauk SSSR Ser. Khim.* **1965**, 1519; L. M. Andronov, Z. K. Maizus, N. M. Emanuel, *Russ. Chem. Bull.* **1965**, *14*, 1489.
[38] L. M. Andronov, Z. K. Maizus, *Izv. Akad. Nauk SSSR Ser. Khim.* **1967**, 519; L. M. Andronov, Z. K. Maizus, *Russ. Chem. Bull.* **1967**, *16*, 504.
[39] W. C. Ketchie, Y.-L. Fang, M. S. Wong, M. Murayama, R. J. Davis, *J. Catal.* **2007**, *250*, 94.
[40] *Modern Aldol Reactions. Vol. 1: Enolates, Organocatalysis, Biocatalysis and Natural Product Synthesis* (Ed.: R. Mahrwald), Wiley-VCH, **2004**.
[41] R. T. Morrison, R. N. Boyd, *Organic chemistry, 6th ed.*, Prentice-Hall Inc., **2002**.
[42] N. Dimitratos, J. A. Lopez-Sanchez, J. M. Anthonykutty, G. Brett, A. F. Carley, R. Ch. Tiruvalam, A. A. Herzing, Ch. J. Kiely, D. W. Knight, G. J. Hutchings, *Phys. Chem. Chem. Phys.* **2009**, *11*, 4952.
[43] O. Novotny, K. Cejpek, J. Velisek, *Czech J. Food Sci.* **2008**, *26*, 117.
[44] E. Díaz, M. E. Sad, E. Iglesia, *ChemSusChem* **2010**, *3*, 1063.
[45] J. Turkevich, P. C. Stevenson, J. Hillier, *J. Phys. Chem.* **1953**, *57*, 670.
[46] J. Turkevich, P. C. Stevenson, J. Hillier, *Discuss. Faraday Soc.* **1951**, *11*, 55.
[47] Gaussian 03, Revision D.01, M. J. Frisch, G. W. Trucks, H. B. Schlegel, G. E. Scuseria, M. A. Robb, J. R. Cheeseman, J. A. Montgomery, Jr., T. Vreven, K. N. Kudin, J. C. Burant, J. M. Millam, S. S. Iyengar, J. Tomasi, V. Barone, B. Mennucci, M. Cossi, G. Scalmani, N. Rega, G. A. Petersson, H. Nakatsuji, M. Hada, M. Ehara, K. Toyota, R. Fukuda, J. Hasegawa, M. Ishida, T. Nakajima, Y. Honda, O. Kitao, H. Nakai, M. Klene, X. Li, J. E. Knox, H. P. Hratchian, J. B. Cross, V. Bakken, C. Adamo, J. Jaramillo, R. Gomperts, R. E. Stratmann, O. Yazyev, A. J. Austin, R. Cammi, C. Pomelli, J. W. Ochterski, P. Y. Ayala, K. Morokuma, G. A. Voth, P. Salvador, J. J. Dannenberg, V. G. Zakrzewski, S. Dapprich, A. D. Daniels, M. C. Strain, O. Farkas, D. K. Malick, A. D. Rabuck, K. Raghavachari, J. B. Foresman, J. V. Ortiz, Q. Cui, A. G. Baboul, S. Clifford, J. Cioslowski, B. B. Stefanov, G. Liu, A. Liashenko, P. Piskorz, I. Komaromi, R. L. Martin, D. J. Fox, T. Keith, M. A. Al-Laham, C. Y. Peng, A. Nanayakkara, M. Challacombe, P. M. W. Gill, B. Johnson, W. Chen, M. W. Wong, C. Gonzalez, J. A. Pople, Gaussian, Inc., Wallingford CT, **2004**.
[48] A. D. Becke, *J. Chem. Phys.* **1993**, *98*, 5648.
[49] T. H. Dunning Jr., and P. J. Hay, in *Modern Theoretical Chemistry, Vol. 3* (Ed.: H. F. Schaefer, III), Plenum, New York, **1976**, pp. 1–28.
[50] B. Mennucci, J. Tomasi, *J. Chem. Phys.* **1997**, *106*, 5151; S. Miertuš, E. Scrocco, J. Tomasi, *Chem. Phys.* **1981**, *55*, 117.

Received: March 12, 2012

Getting the balance right: The product distribution observed during the liquid-phase partial oxidation reaction of glycerol is discussed in terms of balance between reactions specifically induced by the presence of a base in the medium and reactions as a result of the specific action of gold nanoparticles as catalyst (see figure). A global reaction scheme supported by a set of mechanistic analyses is proposed.

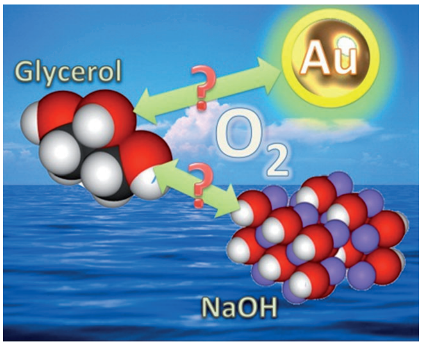

E. Skrzyńska, J. Ftouni, J.-S. Girardon, M. Capron, L. Jalowiecki-Duhamel, J.-F. Paul, F. Dumeignil**

■■–■■

Quasi-Homogeneous Oxidation of Glycerol by Unsupported Gold Nanoparticles in the Liquid Phase